 Human Molecular Genetics, 2002, Vol. 11, No. 15 1731–1742

Pioglitazone improves the phenotype and molecular defects of a targeted *Pkd1* mutant

Satoru Muto[1], Atsu Aiba[2], Yuichirou Saito[3], Kazuki Nakao[4], Kenji Nakamura[5], Kyoichi Tomita[1], Tadaichi Kitamura[1], Masahiko Kurabayashi[3], Ryozo Nagai[6], Eiji Higashihara[7], Peter C. Harris[8], Motoya Katsuki[9] and Shigeo Horie[1,7,*]

[1]Department of Urology, The University of Tokyo, Tokyo 113-8655, Japan, [2]Department of Cell Biology, Kobe University, Kobe 650-0017, Japan, [3]Second Department of Internal Medicine, Gunma University, Maebashi 371-8511, Japan, [4]Riken, Center for Developmental Biology, Kobe 650-0047, Japan, [5]Mitsubishi Kasei Institute of Life Sciences, Machida 194-8511, Japan, [6]Department of Cardiovascular Medicine, The University of Tokyo, Tokyo 113-8655, Japan, [7]Department of Urology, Kyorin University, Mitaka 181-8611, Japan, [8]Department of Nephrology, Mayo Clinic, Rochester, MN 55905, USA and [9]National Institute for Basic Biology, Okazaki National Research Institutes, Okazaki 444–8585, Japan

Received March 28, 2002; Revised and Accepted May 24, 2002

Mutations of either *PKD1* or *PKD2* are associated with autosomal dominant polycystic kidney disease (ADPKD). The molecular function of the gene product of *PKD1*, polycystin-1, *in vitro* has been elucidated recently, but the molecular pathological consequences of the loss of polycystin-1 *in vivo* have remained unclear. We have generated a mouse with a targeted deletion of exons 2–6 of *Pkd1* to study the molecular defects in *Pkd1* mutants. Homozygote embryos (*Pkd1*$^{-/-}$) developed hydrops, cardiac conotruncal defects and renal cystogenesis. Total protein levels of β-catenin in heart and kidney and c-MYC in heart were decreased in *Pkd1*$^{-/-}$ embryos. In the kidneys of *Pkd1*$^{-/-}$, the expression of E-cadherin and PECAM in basolateral membranes of renal tubules was attenuated, and tyrosine phosphorylation of epidermal growth factor receptor and Gab1 were constitutively enhanced when cystogenesis started on embryonic day (E) 15.5–16.5. Maternally administered pioglitazone, a thiazolidinedione compound, resolved these molecular defects of *Pkd1*$^{-/-}$. Treatment with pioglitazone improved survival of *Pkd1*$^{-/-}$ embryos and ameliorated the cardiac defects and the degree of renal cystogenesis. Long-term treatment with pioglitazone improved the endothelial function of adult *Pkd1*$^{+/-}$. These data indicated that molecular defects observed in *Pkd1*$^{-/-}$ embryos contributed to the pathogenesis of ADPKD and that thiazolidinediones had a compensatory effect on the pathway affected by the loss of polycystin-1. Pathways activated by thiazolidinediones may provide new therapeutic targets in ADPKD.

INTRODUCTION

Autosomal dominant polycystic kidney disease (ADPKD) causes epithelial cysts, aneurysms, cardiac valvular insufficiency, hypertension and renal insufficiency (1). Mutations in *PKD1* (2) and *PKD2* (3) are present in ADPKD. The *PKD1* and *PKD2* genes encode polycystin-1 and polycystin-2, respectively. Recently, the molecular function of polycystin-1 *in vitro* has been reported. Interaction of polycystin-1 and -2 results in the formation of calcium-permeable non-selective cation channels (4). Overexpression of *PKD1* inhibits apoptosis and promotes spontaneous tubulogenesis in MDCK cells (5). Targeted disruption of the murine ortholog of *Pkd1* has helped elucidate the function of its protein product (6–10). Homozygotes of *Pkd1* mutants, including *Pkd1*^{L} (6), *Pkd1*$^{del17–21geo}$ (7), *PKD1*^{null} (8) and *Pkd1*^{del34} (9), die *in utero* and develop renal and pancreatic cysts. Some homozygous *Pkd1* mutants have cardiac conotruncal defects (7), vascular fragility associated with focal hemorrhage, or both (6–8). Heterozygous *Pkd1* mutants develop adult-onset polycystic kidney as well as liver and pancreatic disease (7,8,10), which largely recapitulates the clinical pattern seen in ADPKD. Cystogenesis in ADPKD features perturbations of polarization and cellular hyperproliferation (11). Cultured ADPKD cells show impaired basolateral trafficking in membrane transport and abnormal localization of E-cadherin (12). The activation of tyrosine kinases mediated by growth

*To whom correspondence should be addressed at: Department of Urology, Kyorin University School of Medicine, 6-20-2, Shinkawa, Mitaka, Tokyo, Japan 181-8611. Fax: +81 422428431; Email: shorie-kkr@umin.ac.jp

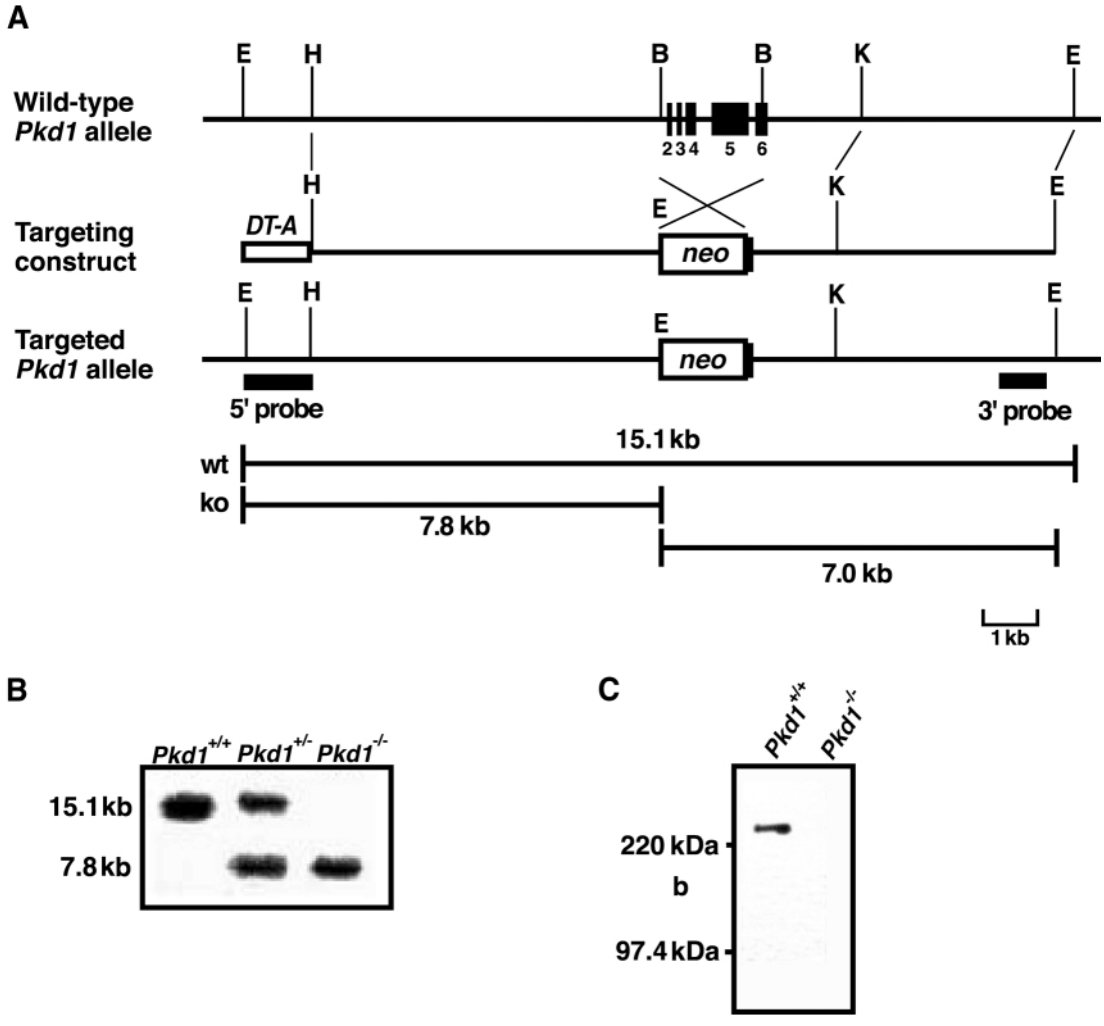

Figure 1. Generation of a targeted disruption of *Pkd1* and its phenotype. (**A**) Structures of wild-type and targeted *Pkd1* alleles. A *Bgl*II fragment containing exon 2–5 and a part of exon 6 was replaced with an MC1 promoter-driven neo-resistant gene. The positions of the 5′ and 3′ external probes are indicated. E, *Eco*RV; B, *Bgl*II; K, *Kpn*I; H, *Hinc*II. (**B**) A southern blot of *Eco*RV-digested DNA from a cross of $Pkd1^{+/-}$ mice hybridized with an external 5′ probe showing the wild-type (15.1 kb) and mutant (7.8 kb) alleles; this result was confirmed with the 3′ external probe (data not shown). (**C**) Western analysis of membrane fractions from E12.5 whole-mouse embryos. A monoclonal antibody (7e12) against the N-terminus of polycystin-1 detected a prominent 460 kDa band in the wild-type allele and was absent in $Pkd1^{-/-}$.

factors such as epidermal growth factor (EGF) (13,14) and hepatocyte growth factor (HGF) (15,16) stimulates a tubular cell to change to a hyperproliferative state. The association of these *in vitro* findings with the phenotypes observed in *Pkd1* mutants has not been fully examined.

We have generated *Pkd1*-mutant mice with a targeted deletion of exon 2–6 to further delineate the molecular defects associated with loss of polycystin-1. In addition, we have explored the possibility of using thiazolidinediones to treat ADPKD.

RESULTS

Generation of $Pkd1^{-/-}$ mice and analysis of the phenotypes

We designed a *Pkd1* targeting vector to replace the *Bgl*II–*Bgl*II fragment including exons 2–5 and part of exon 6, which contains the neomycin-resistance gene (Fig. 1A). Embryonic stem (ES) cell clones containing the correct replacement (Fig. 1B) were injected into C57BL/6J blastocysts, and germline transmission was achieved. Heterozygous ($Pkd1^{+/-}$) mice were crossed to produce homozygous ($Pkd1^{-/-}$) offspring. The targeted *Pkd1* alleles underwent a frameshift. By western blotting, we confirmed the absence of polycystin-1 expression in $Pkd1^{-/-}$ (Fig. 1C). Analysis of staged embryos showed that on embryonic day (E) 14.5, $Pkd1^{-/-}$ embryos started dying *in utero* (Table 1). $Pkd1^{-/-}$ embryos exhibited hydrops fetalis and focal hemorrhages (Fig. 2B). The hearts of $Pkd1^{-/-}$ embryos at E12.5 showed hemorrhagic pericardial effusion and had a double-outlet right ventricle (DORV) (Fig. 2E). In the $Pkd1^{-/-}$ kidney, progressive renal cystogenesis started around E15.5. At E18.5, the renal parenchyma of $Pkd1^{-/-}$ had numerous cysts (Fig. 3B).

β-Catenin and c-MYC decreased in *Pkd1*$^{-/-}$ heart

Previous studies showed that the C-terminal region of polycystin-1 protects soluble β-catenin from degradation (17). We examined the amount of total β-catenin in the hearts at E12.5. The western blot demonstrated that the β-catenin protein level was 39% lower in *Pkd1*$^{-/-}$ than in wild-type (β-catenin protein level normalized by β-actin, arbitrary ratio; wild-type; 0.72 ± 0.28, $n = 5$; *Pkd1*$^{-/-}$; 0.44 ± 0.20, $n = 5$, $P = 0.0047$) (Fig. 2G). The protein level of c-MYC, a target molecule of β-catenin (18), was 75% lower in *Pkd1*$^{-/-}$ heart than in wild-type heart (c-MYC protein level normalized by β-actin, arbitrary ratio; wild-type, 0.68 ± 0.18, $n = 3$; *Pkd1*$^{-/-}$, 0.13 ± 0.13, $n = 3$, $P = 0.021$) (Fig. 2G).

Molecular defects in *Pkd1*$^{-/-}$ kidney

We examined the amount of total β-catenin in the kidneys at E16.5. The β-catenin protein level was 34% lower in *Pkd1*$^{-/-}$ than in wild-type (β-catenin protein level normalized by β-actin, arbitrary ratio; wild-type, 0.98 ± 0.16, $n = 3$; *Pkd1*$^{-/-}$, 0.65 ± 0.04, $n = 3$, $P = 0.020$) (Fig. 3E). However, the protein level of c-MYC was comparable between wild-type and *Pkd1*$^{-/-}$ kidney (c-MYC protein level normalized by β-actin, arbitrary ratio; wild-type, 0.56 ± 0.22, $n = 3$; *Pkd1*$^{-/-}$, 0.42 ± 0.27, $n = 3$, $P = 0.51$) (Fig. 3E). To see if the loss of polycystin-1 affected the expression of adherens junction (AJ) proteins *in vivo*, we examined the expression of AJ proteins in renal tubules at E16.5. Anti-E-cadherin antibodies stained the basolateral membranes of the wild-type renal tubules (Fig. 4A). In *Pkd1*$^{-/-}$ tubules, the basolateral staining of E-cadherin was less prominent (Fig. 4B and G). The western blot showed that the total protein level of E-cadherin was lower in *Pkd1*$^{-/-}$ kidney than in wild-type kidney (Fig. 4H). In developing cysts, the height of an individual cyst epithelial cell was shorter compared to that of a normal tubule; and the basolateral expression of E-cadherin was lost to a remarkable extent (Fig. 4G). Basolateral expression of PECAM-1 (CD 31), another component of AJ, was also reduced in *Pkd1*$^{-/-}$ tubules (Fig. 4D and E) in association with the decrease in protein level (Fig. 4H). These data suggest that the loss of polycystin-1 affected the metabolism of AJ proteins. To investigate whether abnormal cell signaling is involved in the activation of EGF receptor (EGFR) and Gab1, an adapter cytoplasmic protein associated with activated EGFR and c-MET (19,20), we examined the phosphorylation status of EGFR and Gab1 in *Pkd1*$^{-/-}$ tubules. Immunohistochemistry with anti-tyrosine phosphorylated EGFR showed the positive staining of cells in renal tubules (Fig. 5B) and cyst epithelial cells (Fig. 5C) in *Pkd1*$^{-/-}$ kidneys at E16.5. On the other hand, tubular cells of wild-type kidney showed much weaker staining (Fig. 5A). The level of tyrosine-phosphorylated Gab1 was greater in *Pkd1*$^{-/-}$ kidneys at E16.5 than in wild-type kidneys, whereas the protein levels of Gab1 were similar (Fig. 5F).

Maternally administered pioglitazone corrected the molecular defects of *Pkd1*$^{-/-}$ embryos

We hypothesized that decreased total protein levels of β-catenin and c-MYC in *Pkd1*$^{-/-}$ embryonic hearts are associated with cardiac abnormalities which, in turn, result in embryonic death in mid-gestation. Recent studies have shown that thiazolidinediones, peroxisome proliferator-activated receptor γ (PPARγ) agonists, affect Wnt signaling by increasing β-catenin levels in the colon of APC mutant mice (21). Thiazolidinediones also upregulate the expression of c-*myc* mRNA in thyroid cancer cells (22). We investigated whether maternally administered pioglitazone (PIO, Takeda Chemical Industries, Ltd, Osaka, Japan), a thiazolidinedione compound, increased the stability of β-catenin and c-MYC levels in the heart and ameliorated the cardiac phenotype, thereby prolonging survival of the *Pkd1*$^{-/-}$ pups. We administered 80 mg/kg/day of PIO, which crosses the placenta, to pregnant *Pkd1*$^{+/-}$ dams during the period of embryonic days 7.5–9.5. The period of embryonic days 7.5–9.5 was chosen because cardiac neural crest cells migrate to form the outflow tract septa within the lateral walls of the aortic sac and the truncus arteriosus at E9.5 (23). Pregnant *Pkd1*$^{+/-}$ dams were given freshly prepared paste food complemented with pioglitazone (PIO) daily, and its complete consumption was confirmed every day. At E16.5, the survival of *Pkd1*$^{-/-}$ embryos was not different between the control group and the PIO-treated group. Six of 51(11.8%) live embryos were *Pkd1*$^{-/-}$ without treatment, whereas 18 of 100 (18%) live embryos were *Pkd1*$^{-/-}$ after PIO treatment ($P = 0.32$, $\chi^2 = 0.98$) (Table 1). However, significantly more *Pkd1*$^{-/-}$ embryos receiving PIO treatment lived to E18.5. At E18.5, only 2 of 68 (2.9%) live embryos were *Pkd1*$^{-/-}$ without treatment, whereas 6 of 41 (15%) live embryos were *Pkd1*$^{-/-}$ after treatment ($P = 0.023$, $c^2 = 5.1$). When PIO was administered to dams during the period 9.5–11.5 p.c., the number of *Pkd1*$^{-/-}$ embryos at E16.5 (2 of 33 total embryos, 6.1%) was lower than among those which had earlier treatment (18 of 100 total

Table 1. Number of embryos examined from *Pkd1*$^{+/-}$ intercrosses at various developmental stages

Embryonic day	Control						PIO 7.5–9.5						PIO 9.5–11.5					
	Pkd1$^{-/-}$		*Pkd1*$^{+/-}$		*Pkd1*$^{+/+}$		*Pkd1*$^{-/-}$		*Pkd1*$^{+/-}$		*Pkd1*$^{+/+}$		*Pkd1*$^{-/-}$		*Pkd1*$^{+/-}$		*Pkd1*$^{+/+}$	
	Alive	(Dead)	Alive	(Dead)	Alive	(Dead)	Alive	(Dead)	Alive	(Dead)	Alive	(Dead)	Alive	(Dead)	Alive	(Dead)	Alive	(Dead)
12.5	31	(2)	67	(4)	24	(2)	14	(3)	32	(2)	9	(1)						
13.5	29	(3)	64	(4)	30	(0)												
14.5	10	(5)	36	(0)	20	(1)												
15.5	4	(6)	30	(0)	27	(1)												
16.5	6	(1)	28	(0)	16	(0)	18	(4)	47	(3)	28	(0)	2	(4)	19	(1)	7	(0)
17.5	1	(10)	17	(1)	15	(0)												
18.5	2	(9)	36	(2)	17	(2)	6	(4)	20	(2)	15	(1)						

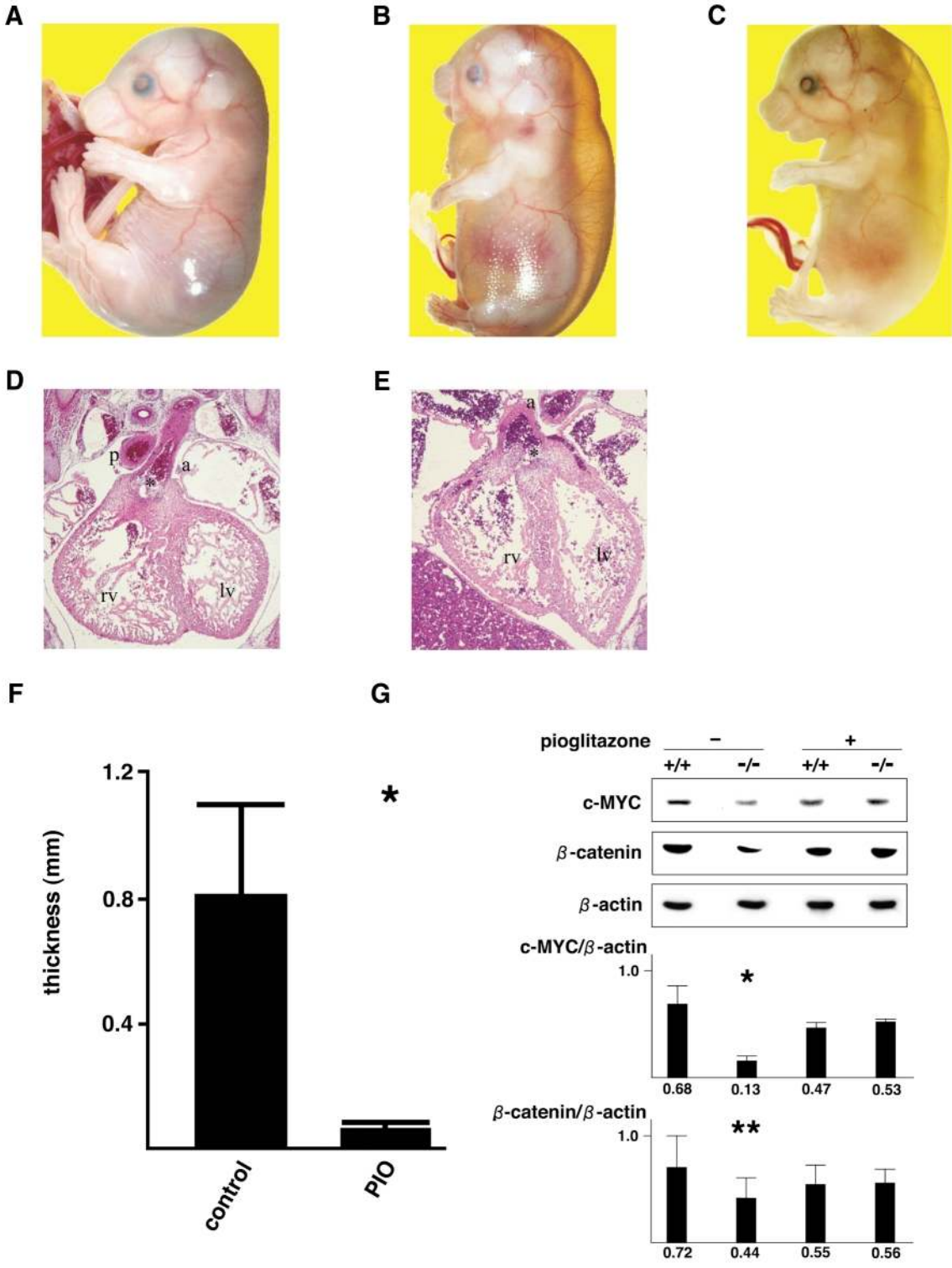

Figure 2. Phenotype of *Pkd1*$^{-/-}$ embryos and the effects of pioglitazone (PIO) treatment. (**A**–**C**) Appearance of *Pkd1*$^{-/-}$ embryos at E16.5: (A) wild-type; (B) *Pkd1*$^{-/-}$; (C) PIO-treated *Pkd1*$^{-/-}$. (**D** and **E**) Transverse section of embryonic heart (E13.5): (D) wild-type; (E) *Pkd1*$^{-/-}$ showing a double-outlet right ventricle (DORV). Aortic valve opens for both left and right ventricle. rv, right ventricle; lv, left ventricle; p, pulmonary artery; a, aorta; *, aortic valve. ×40. (**F**) Effect of PIO on subcutaneous edema in *Pkd1*$^{-/-}$ embryos (E16.5). *, $P < 0.005$, compared with control, *t*-test, mean ± SD. (**G**) Western blot analysis of c-MYC and β-catenin protein expression in embryonic hearts (E12.5). Individual protein levels are normalized by the expression of β-actin. +/+, wild-type; −/−, *Pkd1*$^{-/-}$. *, $P < 0.05$; **, $P < 0.005$; *t*-test, relative to untreated wild-type, mean ± SD.

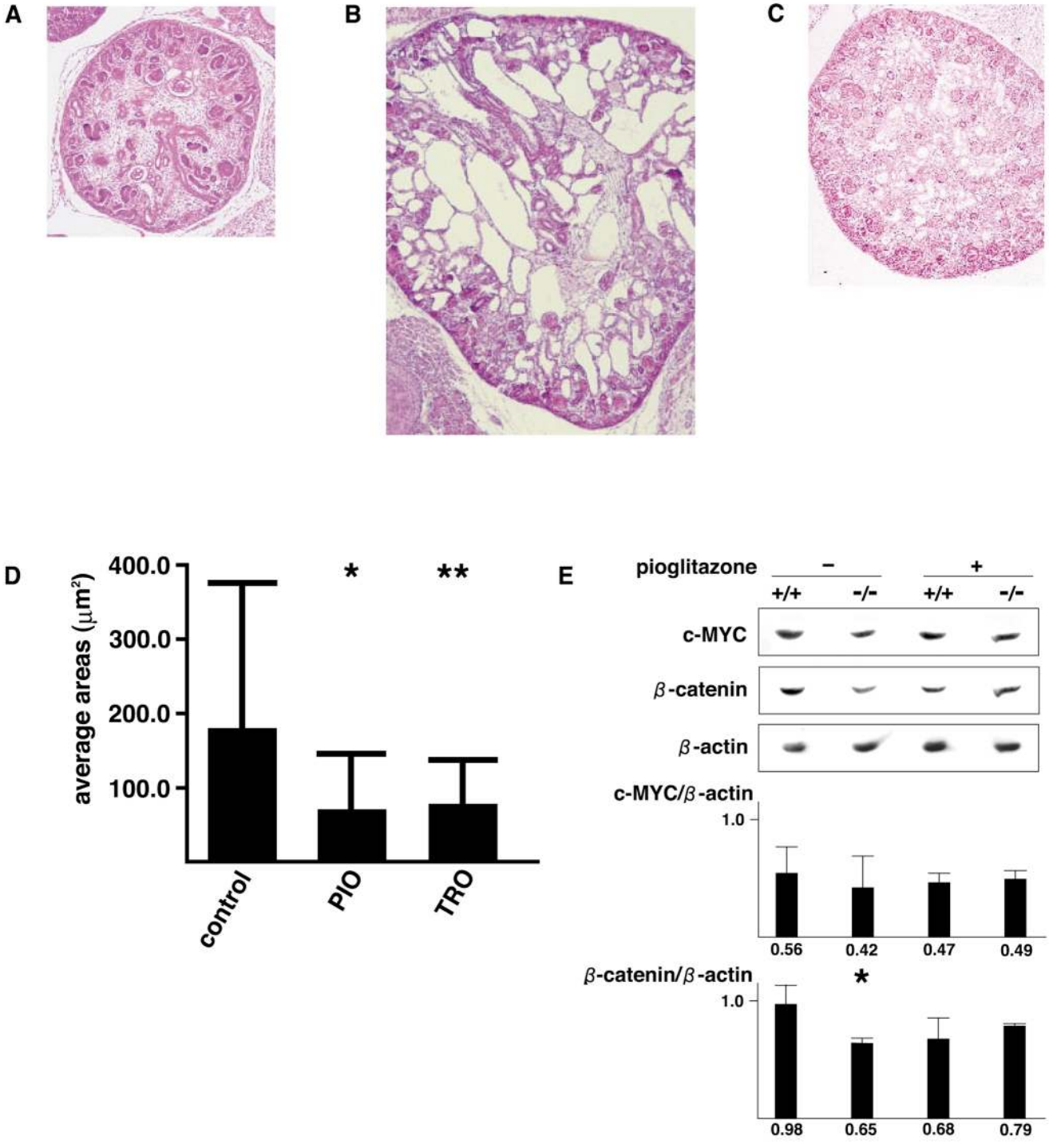

Figure 3. PIO treatment inhibited cystogenesis in $Pkd1^{-/-}$ embryonic kidneys. (**A**–**C**) Embryonic kidney at E18.5 (H&E; magnification ×40). (A) Wild-type; (B) $Pkd1^{-/-}$, (C) PIO-treated $Pkd1^{-/-}$. (**D**) Effects of PIO treatment on the average area of individual cystic lesions on the largest transverse section of an embryonic $Pkd1^{-/-}$ kidney. PIO, pioglitazone; TRO, troglitazone. *, $P < 0.0001$; **, $P < 0.0005$, relative to control, as determined by ANOVA with *post hoc* Bonferroni-corrected *t*-test, mean ± SD. (**E**) Western blot analysis of c-MYC and β-catenin protein expression in embryonic kidney (E16.5). Individual protein levels are normalized by the expression of β-actin. +/+, wild-type; −/− $Pkd1^{-/-}$. *, $P < 0.05$, *t*-test, relative to untreated wild-type, mean ± SD.

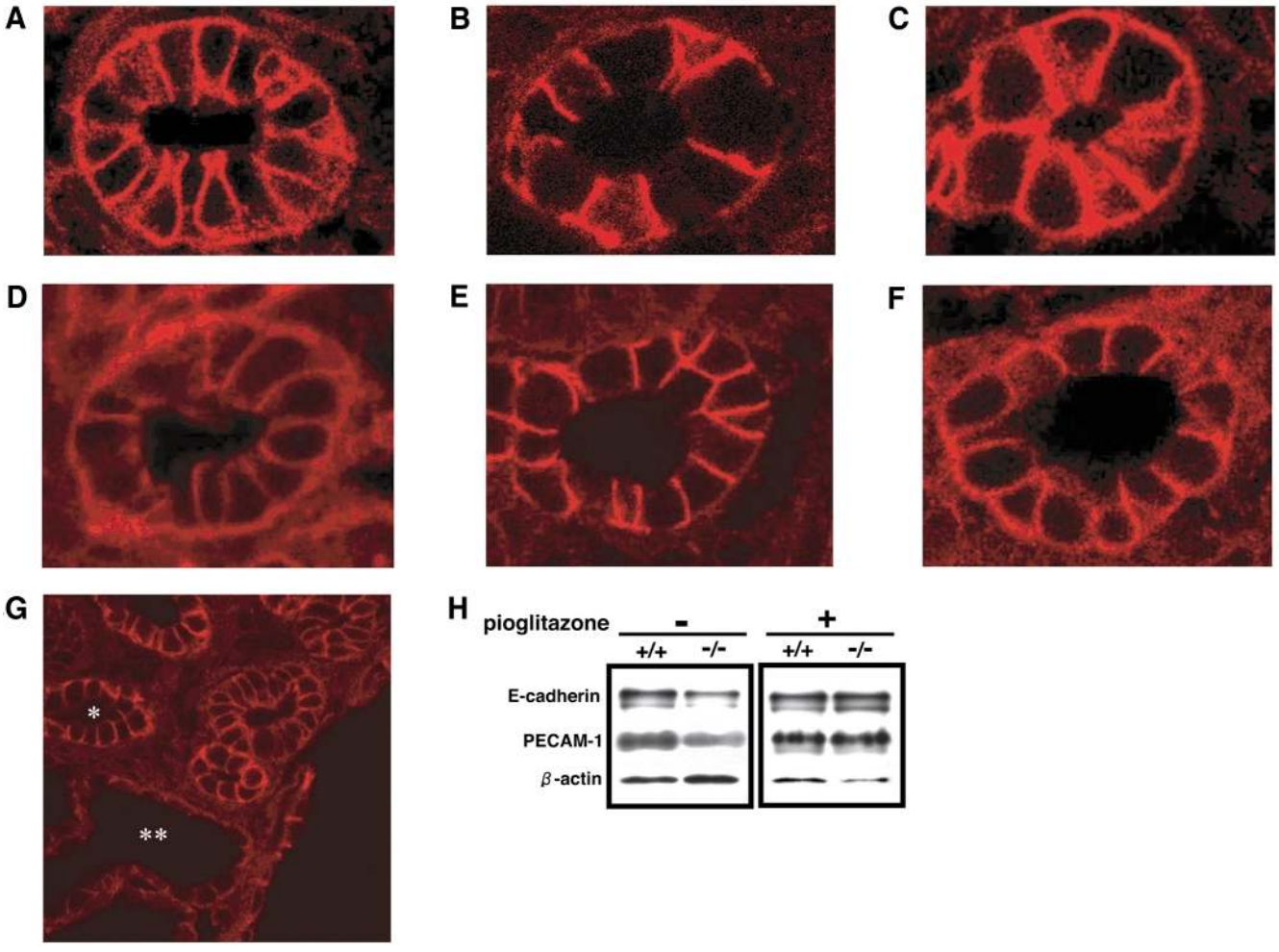

Figure 4. Decrease in the expression of adherens junction proteins in *Pkd1*$^{-/-}$ kidneys and the effect of PIO treatment. (**A**–**G**) Expression of adherens junction proteins in renal tubules (E16.5). (A–C and G) Staining for E-cadherin, and (D–F) staining for PECAM-1, where (A and D) is wild-type, (B,E and G) is *Pkd1*$^{-/-}$, and (C and F) is PIO-treated *Pkd1*$^{-/-}$ (magnification × 600). A non-dilated tubule (*) started losing basolateral E-cadherin expression. In a developing cyst (**), the height of a cyst epithelial cell was shorter compared to that of a normal tubule. Cyst epithelium lost the expression of E-cadherin to a remarkable start. (**H**) Western blot analysis of E-cadherin and PECAM-1 protein expression in embryonic kidney (E16.5). +/+, wild-type; −/−, *Pkd1*$^{-/-}$.

embryos, 18%), although the difference was not statistically significant ($P = 0.096$, $\chi^2 = 2.8$) (Table 1). PIO-treated *Pkd1*$^{-/-}$ embryos had less subcutaneous edema than the untreated embryos (Fig. 2B and C). Edema was quantified by measuring the thickness of the subcutaneous tissue of *Pkd1*$^{-/-}$ embryos at E16.5 in the control and PIO-treated groups (control, 820 ± 282 μm; PIO-treated, 59.4 ± 12.0 μm, $P = 0.0011$) (Fig. 2F). Cardiac DORV, examined at E16.5, was not found in four live *Pkd1*$^{-/-}$ embryos from the PIO-treated dams, but did occur in four of five live control *Pkd1*$^{-/-}$ embryos ($P = 0.016$, $\chi^2 = 5.76$). In PIO-treated embryos, the levels of β-catenin and c-MYC in the heart at E12.5 were similar in *Pkd1*$^{-/-}$ and wild-type embryos (Fig. 2G). These results indicated that maternal treatment with PIO corrected the molecular defects and reduced the cardiac defects of the *Pkd1*$^{-/-}$ embryos. PIO treatment significantly reduced the level of renal cystogenesis (Fig. 3B and C). PIO-treated *Pkd1*$^{-/-}$ kidneys showed only slightly dilated renal tubules even at E18.5, with much less cystic enlargement as compared to untreated *Pkd1*$^{-/-}$ kidneys. Another thiazolidinedione compound, troglitazone (TRO, Sankyo Co., Ltd, Tokyo, Japan) (2 g/kg/day administered during 7.5–9.5 p.c.) had a similar effect on the inhibition of renal cystogenesis. The average area of individual renal cysts at E18.5 was significantly smaller in PIO- and TRO-treated *Pkd1*$^{-/-}$ embryos than in untreated *Pkd1*$^{-/-}$ controls (control, 124 cysts/5 kidneys; average area of individual renal cysts 179 ± 197 μm^2; PIO-treated, 73 cysts/5 kidneys; 71 ± 76 μm^2, $P < 0.0001$ versus control; TRO-treated, 42 cysts/3 kidneys; 81 ± 57 μm^2, $P = 0.0003$ versus control) (Fig. 3D). In PIO-treated embryos, the levels of β-catenin and c-MYC in the kidneys at E16.5 were similar in *Pkd1*$^{-/-}$ and wild-type (β-catenin protein level normalized by β-actin, arbitrary ratio; wild-type, 0.68 ± 0.18, $n = 3$; *Pkd1*$^{-/-}$, 0.79 ± 0.02, $n = 3$, $P = 0.24$; c-MYC protein level normalized by β-actin, arbitrary ratio; wild-type, 0.47 ± 0.08, $n = 3$; *Pkd1*$^{-/-}$, 0.49 ± 0.08, $n = 3$, $P = 0.92$) (Fig. 3E). Expression of AJ proteins in renal tubules was maintained in PIO-treated *Pkd1*$^{-/-}$ embryos (Fig. 4C,F and G). Enhanced tyrosine

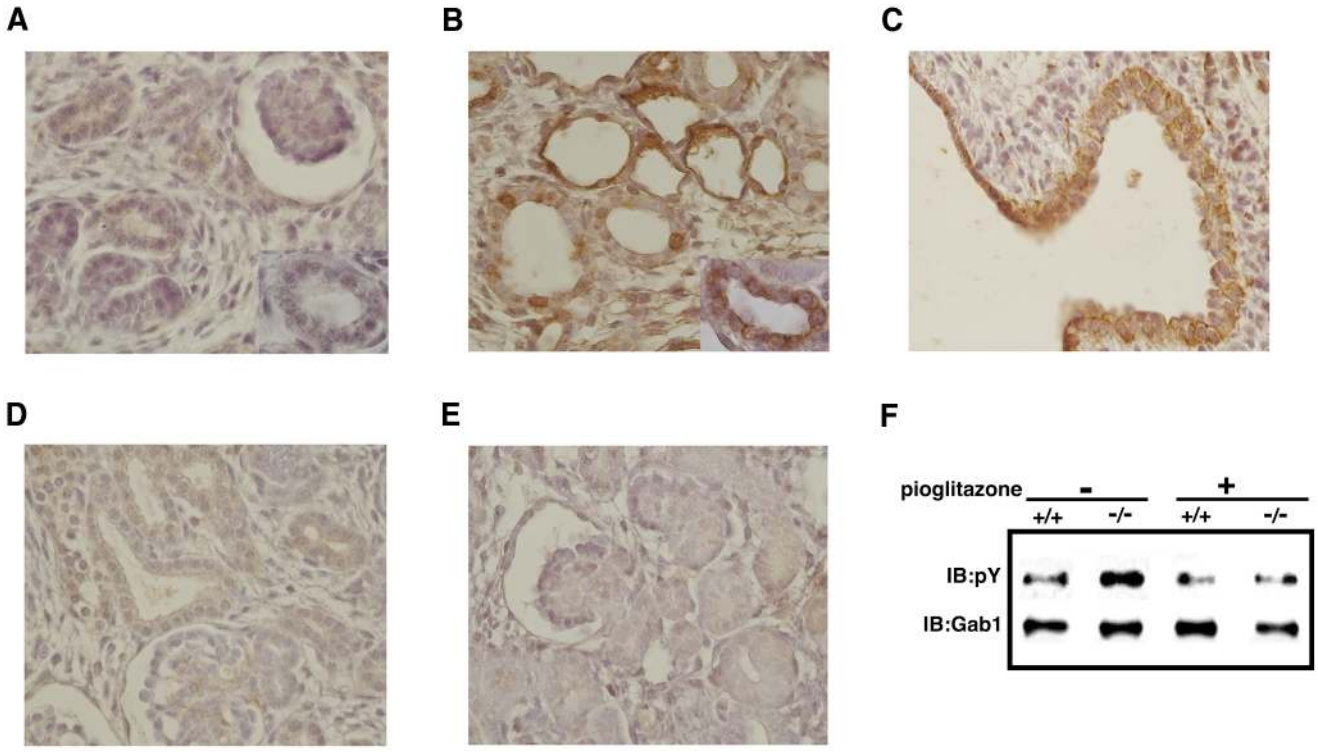

Figure 5. Activation of EGFR and Gab1 in $Pkd1^{-/-}$ kidneys and the effect of PIO treatment. (**A**–**E**) Immunohistochemistry determination of tyrosine-phosphorylated EGFR in embryonic kidneys at E16.5. Activated EGFR was expressed in the cells of renal tubules (B) and cyst epithelium (C) in $Pkd1^{-/-}$, while weak staining for activated EGFR was demonstrated in wild-type littermates (A). The expression of activated EGFR was inhibited in tubules of PIO-treated $Pkd1^{-/-}$ (E), which was comparable with wild-type littermates (D). Magnification × 600, inset × 2500). (**F**) Immunoprecipitation and western blot analysis of the expression and tyrosine phosphorylation of Gab1 in embryonic kidney (E16.5). +/+, wild-type, $Pkd1^{-/-}$.

phosphorylation of EGFR and Gab1 observed in $Pkd1^{-/-}$ embryonic kidneys was not seen in PIO-treated $Pkd1^{-/-}$ (Fig. 5D–F).

Pioglitazone improved endothelial function in *Pkd1*$^{+/-}$ adults

Impaired endothelium-dependent relaxation has been demonstrated previously in small subcutaneous resistance vessels obtained from patients with ADPKD (24). To investigate whether endothelium-dependent relaxation was reduced also in large vessels, acetylcholine (ACh)-induced endothelium-dependent relaxation was measured in the aorta obtained from 30-week-old adult $Pkd1^{+/-}$ mice. The maximum relaxation rate (E_{max}) induced by ACh at the concentration of 10^{-5} M was significantly lower in $Pkd1^{+/-}$ than in wild-type (wild-type, $98.6 \pm 2.40\%$, $n = 5$; $Pkd1^{+/-}$, $84.8 \pm 5.80\%$, $n = 5$, $P = 0.0011$) (Fig. 6A). There was no difference in the sodium nitroprusside-induced (E_{max}) between $Pkd1^{+/-}$ and wild-type (data not shown). We next repeated this study in 10-month-old $Pkd1^{+/-}$ mice fed with PIO (40 mg/kg/day) and without PIO for the last 6 months to determine whether long-term treatment with PIO improves endothelial function. The systolic blood pressure of PIO-treated $Pkd1^{+/-}$ mice was not different from that of untreated $Pkd1^{+/-}$ mice untreated control, 119 ± 10 mmHg; PIO-fed, 108 ± 7 mmHg, $P = 0.33$). However, comparing the animal growth rate, body weight was significantly decreased in PIO-fed $Pkd1^{+/-}$ mice compared to untreated $Pkd1^{+/-}$ mice untreated control, 37.0 ± 0.7 g; PIO-fed, 33.3 ± 1.3 g, $P = 0.017$). PIO-treated $Pkd1^{+/-}$ mice showed a significantly increased E_{max} compared to untreated $Pkd1^{+/-}$ mice (control, $72.9 \pm 7.99\%$, $n = 7$; PIO-treated, $96.8 \pm 2.50\%$, $n = 7$, $P = 0.027$) (Fig. 6B). Nitric oxide (NO) produced in vascular endothelium predominantly mediates ACh-mediated relaxation of the aorta (25). Indeed, the NO synthase inhibitor *N*ω-nitro-L-arginine methylester completely abolished ACh-induced aortic relaxation in both groups (data not shown). Urinary concentration and total daily excretion of NOx were significantly lower in 30-week-old $Pkd1^{+/-}$ mice than in wild-type mice (concentration (mol/l): wild-type, 15.8 ± 7.44, $n = 11$; $Pkd1^{+/-}$, 9.31 ± 5.63, $n = 11$, $P = 0.032$) (total excretion (μM/day): wild-type, 2.44 ± 0.83, $n = 11$; $Pkd1^{+/-}$, 1.58 ± 0.78, $n = 11$, $P = 0.021$) (Fig. 6C). PIO treatment increased the urinary excretion of NOx in 10-month-old $Pkd1^{+/-}$ mice by 98% (μM/day: control, 1.00 ± 0.31, $n = 7$; PIO-treated, 1.98 ± 0.88, $n = 6$, $P = 0.0019$) (Fig. 6D). These data indicated that PIO improved the endothelial function of adult $Pkd1^{+/-}$ mice, presumably by increasing the production of NO.

DISCUSSION

We have generated *Pkd1*-mutant mice by targeted disruption of exon 2–6, which resulted in a frameshift. The phenotype of a $Pkd1^{-/-}$ embryo in this study was almost identical to those of

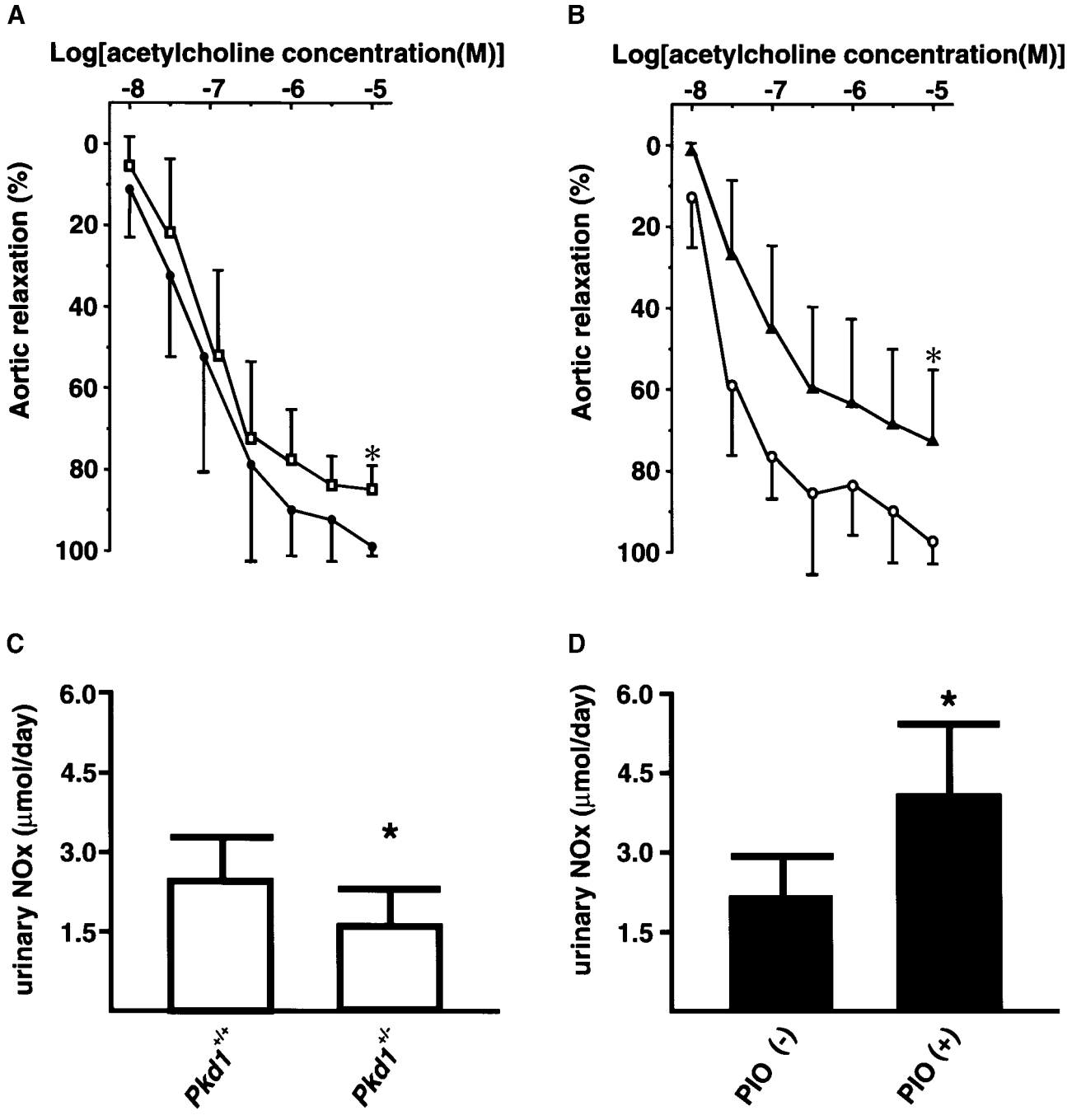

Figure 6. Long-term PIO treatment improved the endothelial dysfunction of adult *Pkd1*$^{+/-}$. (**A** and **B**) Acetylcholine-induced relaxation curve of phenylephrine-precontracted aortic rings. (A) Comparison of wild-type (●) ($n=5$) and *Pkd1*$^{+/-}$ (□) ($n=5$), 30-week-old mice. *, $P<0.005$, *t*-test, relative to wild-type, mean ± SD. (B) Effect of long-term PIO treatment in *Pkd1*$^{+/-}$ adult, 10-month-old mice. Comparison of untreated control (▲) ($n=7$) and PIO-treated (○) ($n=7$). *, $P<0.05$, *t*-test, relative to untreated control, mean ± SD. (**C** and **D**) Amount of NO_x excreted in urine. (C) Comparison of wild-type (*Pkd1*$^{+/+}$) ($n=11$) and *Pkd1*$^{+/-}$ ($n=11$), 30-week-old mice. *, $P<0.05$, *t*-test, relative to wild-type, mean ± SD. (D) Effect of long-term PIO treatment in *Pkd1*$^{+/-}$ adult, 10-month-old mice. PIO(−), untreated control ($n=7$); PIO (+), PIO-treated ($n=6$). *, $P<0.05$, *t*-test, relative to untreated control, mean ± SD.

Pkd1^{L} (6), *Pkd1*$^{del17-21geo}$ (7) and *Pkd1*^{null} (8). Among mutants with a C57BL/6-129 background (Table 2), *Pkd1*$^{L/L}$ has the most severe disease, judging by its embryonic lethality, since it does not survive to E16.5. Mutant polycystin-1 of *Pkd1*$^{L/L}$, L3946*, is much longer than the truncated proteins created by a frameshift in *Pkd1*$^{null/null}$ and *Pkd1*$^{-/-}$. Thus the relationship between disease phenotype and severity and the length of the respective mutant polycystin-1 is not linear.

We then went on to demonstrate biochemical defects in these animals and the effects of a potential treatment. First, we found

that there were decreased levels of β-catenin and c-MYC protein in *Pkd1*$^{-/-}$ embryonic hearts which had conotruncal defects. Cardiac neural crest cells contribute to the development of the proper outflow tract septation (26). In a mouse model of conotruncal heart defects, *Splotch*, Wnt signaling is reduced in cardiac neural crest cells (27). Previous studies showed that Wnt signaling regulates the stability of β-catenin (reviewed in 28), and the C-terminal portion of polycystin-1 protects soluble β-catenin from degradation (17). Present findings suggest that polycystin-1 might play an essential role in the cardiac conotruncal development by modulating the expression of β-catenin and c-MYC. Treatment with maternally administered PIO often corrected the conotruncal defects and increased the levels of β-catenin and c-MYC compared to those of wild-type littermates. The targeted disruption of retinoic X receptors (RXRs) α causes conotruncal defects (29), almost identical to the cardiac phenotype of *Pkd1*$^{-/-}$. PPARγ forms heterodimers with RXRs, which then bind to PPAR-responsive elements (PPRE) in the promoters of PPAR target genes (30). Since no DORV was observed in PIO-treated *Pkd1*$^{-/-}$ embryos, transcriptional regulation by PPRE may have a compensatory effect on the development of cardiac conotruncal defects in response to loss of polycystin-1.

The kidneys of *Pkd1*$^{-/-}$ embryos showed the following molecular defects: decreased levels of β-catenin, perturbation of basolateral expression of AJ proteins in tubules, and enhanced tyrosine phosphorylation of EGFR and Gab1. Recent studies suggest that an aberrant β-catenin signaling pathway may be one of the cellular defects in cystogenesis. Transgenic mice that overproduce an oncogenic form of β-catenin in the epithelial cells of the kidneys develop severe polycystic lesions in the glomeruli, proximal and distal tubules and collecting ducts (31). Mice deficient in the *Bcl-2* gene (*Bcl-2*$^{-/-}$) develop polycystic kidney disease (32), and the epithelial cells that form the cysts in the *Bcl-2*$^{-/-}$ mice accumulate β-catenin in their nuclei (33). These data clearly demonstrate that increased transcriptional activity induced by β-catenin in nuclei mediates renal cystogenesis which features cellular hyperproliferation and dedifferentiation (11). Several lines of evidence suggest that the β-catenin signaling pathway is a downstream effector of polycystin-1. Polycystin-1 has been found in a complex containing E-cadherin and catenins (34). The C-terminal tail of polycystin-1 protects cytoplasmic β-catenin from degradation by the proteasome, and activates Wnt/β-catenin-dependent transcription (17). In differentiated epithelia, the amount of β-catenin is tightly regulated and its steady-state level outside the cadherin–catenin complex is low. The loss of polycystin-1 might disrupt a polycystin-1–E-cadherin–β-catenin complex at the adherens junctions and might alter the cellular metabolism of β-catenin. Therefore, the decreased amounts of β-catenin in *Pkd1*$^{-/-}$ kidneys seen in this study would not necessarily exclude the possibility that transcriptional activity mediated by β-catenin in the nuclei was increased.

Cyst epithelium features a hyperproliferative state and loss of cellular polarity (11). In a developing cyst in *Pkd1*$^{-/-}$ kidneys, the cyst epithelial cells were shorter in height compared to normal tubular cells and there was a remarkable decrease in the expression of E-cadherin (Fig. 4G). The precise relationship between the disruption of cell polarity and the induction of cell proliferation remains unclear. However, it has recently been reported that ErbB2 affects cell polarity and induces cell proliferation in growth-arrested mammary acini (35). This report emphasizes that uncontrolled activation of tyrosine kinase-mediated signaling leads to the modification of cytoarchitecture. Hence, the decrease in AJ proteins and constitutive activation of EGFR and Gab1 in the *Pkd1*$^{-/-}$ kidney might be mutually associated with the loss of polycystin-1. As mentioned before, molecular defects were corrected in the kidney of PIO-treated *Pkd1*$^{-/-}$ embryos. The mechanisms remain unclear. However, since the EGFR tyrosine kinase inhibitor EKI-785 inhibits renal cystogenesis in *bpk* mice (36), the effect of PIO on the quenching of tyrosine phosphorylation of EGFR and Gab1 might play a significant role in the prevention of renal cystogenesis in *Pkd1*$^{-/-}$. Recent studies show that polycystin-1 is targeted to the basolateral membrane, where it complexes with polycystin-2, which is either in the plasma membrane or in the endoplasmic reticulum in close apposition to the plasma membrane. Hanaoka *et al.* (4) have found that co-expression and co-assembly of the two polycystins induce a novel cell-surface cation channel activity. Gonzalez-Perrett *et al.* (37) have reported the first direct evidence that polycystin-2 is indeed a cation channel. Recently, Koulen *et al.* (38) have shown that polycystin-2 behaves as a calcium-activated, high-conductance endoplasmic reticulum channel that is permeable to divalent cations *in vivo.* They demonstrated that C-terminal truncation or the introduction of a disease-causing missence mutation led to the loss of intracellular calcium-release signals. Thus they propose that ADPKD results from the loss of a regulated intracellular calcium-release signaling mechanism (38). These studies show that activation of the complex of polycystins results in increased local [Ca^{2+}]. Whether PIO compensates for the signaling pathway of polycystin-1 as being mediated by Ca^{2+} is an intriguing question, and warrants further studies.

Table 2. Mutant polycystin-1 and disease phenotype

Mutant	mRNA	Hydrops fetalis	Polyhydramnios	Hemorrhage	DORV	Renal cysts	Alive at E16.5[a]	Strain	Ref.
Pkd1$^{-/-}$	Exon 1	Y	Y	Y	Y	E15.5	11%	C57BL/6-129	
Pkd1^{null}	Exon 1–4	Y	Y	ND	ND	E15.5	21%	C57BL/6-129	8
Pkd1$^{del17–21geo}$	Exon 1–16	Y	ND	Y	Y	ND	0%	129	7
Pkd1^{del34}	Exon 1–34	ND	ND	ND	ND	E15.5	ND	C57BL/6-129	9
Pkd1^{L}	Exon 1–43	Y	ND	Y	ND	E14.5	0%	C57BL/6-129	6

DORV, double outlet of right ventricle; Y, presence of a phenotype; ND, not described in the reference.
[a]% homozygotes out of total embryos.

Expression of polycystin-1 in vascular smooth muscle cells and in endothelium has been previously reported (39,40). Hypertension and vascular disease develop in patients with ADPKD well before renal function starts to decline. A previous study (24) showed that endothelial dysfunction was present in small-resistance vessels obtained from normotensive ADPKD patients and that eNOS impairment in ADPKD endothelium may be responsible. In this study, adult heterozygous mice revealed the subtle endothelial dysfunction and the defective production of NOx. Moreover, PIO improved endothelial function in older adult heterozygotes and increased NOx production. Our data suggest that adult heterozygous mice might recapitulate the endothelial dysfunction seen in human subjects. The effect of PIO in adult heterozygous *Pkd1* mutants may indicate that thiazolidinediones improve the endothelial dysfunction in ADPKD patients.

In summary, $Pkd1^{-/-}$ embryos had specific molecular defects, including decreased levels of total β-catenin in the developing hearts and kidneys, decreased levels of c-MYC in the developing hearts, abnormal metabolism of E-cadherin and PECAM-1 in maturing renal tubules, and enhanced tyrosine phosphorylation of EGFR and Gab1 in the developing kidneys. Maternally administered PIO at 7.5–9.5 p.c. corrected these molecular abnormalities and ameliorated the resulting phenotypes. Long-term treatment with pioglitazone improved the endothelial function in adult $Pkd1^{+/-}$ mice. We propose that these molecular defects contribute to the phenotype of ADPKD. The effects of thiazolidinediones on the molecular pathogenesis of ADPKD warrant further studies.

METHODS

Generation of $Pkd1^{-/-}$ (del2–6) mice

We screened a 129/sv mouse genomic library (Stratagene, La Jolla, CA, USA) with the use of mouse *Pkd1* cDNA fragments (41, Gene bank accession # NM_013630). To generate the targeting construct, we subcloned a 10.2 kb *Hinc*II–*Kpn*I fragment containing exons 2–6 into pBluescript (Stratagene). A 1.9 kb *Bgl*II–*Bgl*II fragment was replaced with a 1.6 kb *Bgl*II–*Bgl*II fragment containing a *neo* gene derived from pMC1*neo*–polyA (Stratagene), and a 1.0 kb fragment containing the DT-A gene for negative selection (a gift from Dr S Aizawa; 42) was inserted at the 5′ end of a 6.5 kb *Hinc*II–*Bgl*II fragment (Fig. 1A). *Bgl*II cuts base position 1547 in exon 6 of *Pkd1* mRNA, and the targeted *Pkd1* alleles resulted in a frameshift. ES cells (E14, 129/sv background, provided by A. Smith) were transfected with the targeting vector as described previously (43). Homologous recombinants were identified by southern blot analysis using a 5′ probe and a 3′ probe as illustrated (Fig. 1A). Two independently targeted ES clones were injected into C57BL/6J blastocysts to generate chimeric mice, and the mutation was transmitted into the germline, resulting in a 129/sv/C57BL/6J background.

Histology and immunofluorescence

For morphological evaluation, mouse tissues were fixed in 4% paraformaldehyde in phosphate-buffered saline (PBS) and embedded in paraffin. Sections (3–5 μm thick) were stained with hematoxylin and eosin (H&E) according to standard protocols. Morphological analysis was performed with a BX51 Olympus microscope (Olympus, Tokyo, Japan). For immunohistochemistry, after deparaffinization through graded xylene and ethanol series, sections were washed in PBS (pH 7.4), and treated with 0.3% hydrogen peroxide in PBS for 30 min. After incubation for 30 min with 10% normal goat serum to block non-specific binding of the antibodies, the sections were incubated with goat polyclonal anti-phospho-EGFR antibody (Santa Cruz Biotechnology, Santa Cruz, CA, USA). After overnight incubation with the primary antibody at 4°C, the sections were reacted with biotinylated secondary antibody for 30 min. Subsequently, the sections were allowed to react for 30 min with avidin–biotin–peroxidase complex (ABC) by using a Vectastain ABS kit (Vector Laboratories, Burlingame, CA, USA) and subjected to the peroxidase reaction with 0.02% 3,3′-diaminobenzidine tetrahydrochloride as a chromogen in PBS constaining 0.007% hydrogen peroxide. For immunofluorescence, frozen sections were subjected to permeabilization with 0.2% Triton X-100 in PBS, blocked with 1% bovine serum albumin (BSA), and stained with anti-PECAM-1 (BD PharMingen, San Diego, CA, USA) or anti-E-cadherin (Takara Shuzo, Otsu, Japan) antibodies. Sections were washed with Tris-buffered saline (TBS)–Triton X-100 (0.01%) and subjected to secondary, Cy™3-conjugated goat anti-rat IgG antibodies (Jackson ImmunoResearch, West Grove, PA, USA), and mounted for confocal laser scanning microscopy (MRC-1024, Bio-Rad, Hercules, CA, USA).

Immunoblotting

Embryonic hearts and kidneys were sonicated in RIPA buffer (20 mM Tris-HCl, 150 mM NaCl, 0.1% sodium dodecyl sulfate (SDS), 1% sodium deoxycholate, 1% Triton X-100, 2 mM EDTA, 50 mM NaF, 1 mM sodium orthovanadate, 20 μg/ml, aprotinin, and 20 μg/ml leupeptin). The protein concentration was determined by bicinchinonic acid assay (Pierce, Rockfold, IL, USA). Proteins were separated by SDS–PAGE and transferred to polyvinylidene difluoride (PVDF) membranes (Bio-Rad). Gels were stained with Coomasie blue to check that comparable amounts of proteins were loaded on the gel and also to check the homogeneity of the transfer. Immunodetection was performed after the membranes were blocked in blocking solutions (20 mM Tris-HCl (pH 7.5), 100 mM NaCl, 0.1% Triton-X, and 3% BSA) and blotted with the following antibodies: anti-c-myc (NeoMarkers, Fremont, CA, USA), anti-β-catenin (BD Transduction Laboratories, Lexington, KY, USA), anti-E-cadherin, anti-PECAM-1, anti-Gab1 (Upstate Biotechnology, Lake Placid, NY, USA), anti-β-actin (Santa Cruz Biotechnology, Santa Cruz, CA, USA), and mouse anti-polycystin-1 (7e12) (44). The filters were washed with TBS/0.1% Triton-X, and immunoreactive bands were visualized with an enhanced chemiluminescence (ECL) blotting system (Amersham Pharmacia Biotech, Uppsala, Sweden). Blots were quantified by densitometric analysis with the NIH Image 1.61/ppc program.

Immunoprecipitation and detection of tyrosine phosphorylation

Pre-cleared total lysates (50–100 μg) from the indicated organs were incubated with 2 μg of anti-Gab1 antibody with protein A–Sepharose (Amersham Pharmacia Biotech, Uppsala, Sweden) at 4°C overnight. Immunocomplexes bound to Sepharose beads were washed with RIPA buffer, resuspended in Laemli sample buffer, and boiled before loading. Proteins were resolved by 7.5% SDS–PAGE and transferred to PVDF membranes (Millipore, Bedford, MA, USA). After blocking, immunodetection was performed with an anti-phosphotyrosine antibody (anti-PY) linked to horseradish peroxidase (RC20; BD Transduction Laboratories, Lexington, KY, USA). Signals were detected by ECL blotting.

Analysis of aortic relaxation in response to acetylcholine

Aortic ring (2 mm long) segments were mounted between two stainless steel wires and placed in an organ bath containing Krebs' bicarbonate solution bubbled with a mixture of 95% O_2 and 5% CO_2. One wire was connected to a force-displacement transducer (UR-50G, Minebea Co., Ltd, Nagano, Japan) (45). The preparation was allowed to equilibrate for 90 min and was then preconstricted by phenylephrine (10^{-7} M). To obtain a dose–response curve for acetylcholine (10^{-8} to 10^{-5} M) and sodium nitroprusside (10^{-10} to 10^{-7} M), agents were added cumulatively to the organ bath. Data are expressed as percentage relaxation of phenylephrine-induced preconstriction.

NO_x (NO_2 and NO_3) assay

Concentrations of NO_2 and NO_3 in urine were measured by an autoanalyzer (TCI-NOX 1000, FIA Instruments Co., Ltd, Tokyo, Japan). Deproteinized urine samples were premixed with carrier solution (0.007% EDTA and 0.03% NH_4Cl). Samples were passed through a cadmium reducer and reacted with Griess reagent (1% sulfonamide and 0.1% *N*-1-naphthyl-ethylene-diamine dihydrochloride in 5% HCl). Absorbance was detected at 540 nm using a flow-through visible spectrophotometer (S/3250, Soma-Kogaku, Tokyo, Japan) (45).

ACKNOWLEDGEMENTS

We thank K. Katsuki and T. Etoh for their excellent technical assistance, Y. Chida and M. Emoto for cell culture work and H. Yoshikura, K. Kurokawa, Y. Asano, T. Fujita, T. Igarashi, S. Sasaki, K. Miyazono, T. Suda, T. Koike and R. Nishinakamura for critical comments on this study. This work was supported in part by grants from the Ministry of Health, Labor and Welfare, and the Ministry of Education, Culture, Sports Science and Technology of Japan.

REFERENCES

1. Gabow, P.A. (1993) Autosomal dominant polycystic kidney disease. *N. Engl. J. Med.*, **329**, 332–342.
2. Hughes, J., Ward, C.J., Peral, B., Aspinwall, R., Clark, K., San Millan, J.L., Gamble, V. and Harris, P.C. (1995) The polycystic kidney disease 1 (PKD1) gene encodes a novel protein with multiple cell recognition domains. *Nat. Genet.*, **10**, 151–160.
3. Mochizuki. T., Wu, G., Hayashi, T., Xenophontos, S.L., Veldhuisen, B., Saris, J.J., Reynolds, D.M., Cai, Y., Gabow, P.A., Pierides, A. *et al.* (1996) PKD2, a gene for polycystic kidney disease that encodes an integral membrane protein. *Science*, **272**, 1339–1342.
4. Hanaoka, K., Qian, F., Boletta, A., Bhunia, A.K., Piontek, K., Tsiokas, L., Sukhatme, V.P., Guggino, W.B. and Germino, G.G. (2000) Co-assembly of polycystin-1 and -2 produces unique cation-permeable currents. *Nature (Lond.)*, **408**, 990–994.
5. Boletta, A., Qian, F., Onuchic, L.F., Bhunia, A.K., Phakdeekitcharoen, B., Hanaoka, K., Guggino, W., Monaco, L. and Germino, G.G. (2000) Polycystin-l, the gene product of PKD1, induces resistance to apoptosis and spontaneous tubulogenesis in MDCK cells. *Mol. Cell.*, **6**, 1267–1273.
6. Kim, K., Drummond, I., Ibraghimov-Beskrovnaya, O., Klinger, K. and Arnaout, M.A. (2000) Polycystin 1 is required for the structural integrity of blood vessels. *Proc. Natl Acad. Sci. USA*, **97**, 1731–1736.
7. Boulter, C., Mulroy, S., Webb, S., Fleming, S., Brindle, K. and Sandford, R. (2001) Cardiovascular, skeletal, and renal defects in mice with a targeted disruption of the *Pkd1* gene. *Proc. Natl Acad. Sci. USA*, **98**, 12174–12179.
8. Lu, W., Shen, X., Pavlova, A., Lakkis, M., Ward, C.J., Pritchard, L., Harris, P.C., Genest, D.R., Perez-Atayde, A.R. and Zhou, J. (2001) Comparison of *Pkd1*-targeted mutants reveals that loss of polycystin-1 causes cystogenesis and bone defects. *Hum. Mol. Genet.*, **10**, 2385–2396.
9. Lu, W., Peissel, B., Babakhanlou, H., Pavlova, A., Geng, L., Fan, X., Larson, C., Brent, G. and Zhou, J. (1997) Perinatal lethality with kidney and pancreas defects in mice with a targetted Pkd1 mutation. *Nat. Genet.*, **17**, 179–181.
10. Lu, W., Fan, X., Basora, N., Babakhanlou, H., Law, T., Rifai, N., Harris, P.C., Perez-Atayde, A.R., Rennke, H.G. and Zhou, J. (1999) Late onset of renal and hepatic cysts in Pkd1-targeted heterozygotes. *Nat. Genet.*, **21**, 160–161.
11. Grantham, J.J. and Calvet, J.P. (2001) Polycystic kidney disease: in danger of being X-rated? *Proc. Natl Acad. Sci. USA*, **98**, 790–792.
12. Charron, A.J., Nakamura, S., Bacallao, R. and Wandinger-Ness, A. (2000) Compromised cytoarchitecture and polarized trafficking in autosomal dominant polycystic kidney disease cells. *J. Cell Biol.*, **149**, 111–124.
13. Wilson, P.D., Du, J. and Norman, J.T. (1993) Autocrine, endocrine and paracrine regulation of growth abnormalities in autosomal dominant polycystic kidney disease. *Eur. J. Cell Biol.*, **61**, 131–138.
14. Lee, D.C., Chan, K.W. and Chan, S.Y. (1998) Expression of transforming growth factor alpha and epidermal growth factor receptor in adult polycystic kidney disease. *J. Urol.*, **159**, 291–296.
15. Horie, S., Higashihara, E., Nutahara, K., Mikami, Y, Okubo, A., Kano, M. and Kawabe, K. (1994) Mediation of renal cyst formation by hepatocyte growth factor. *Lancet*, **344**, 789–791.
16. Takayama, H., LaRochelle, W.J., Sabnis, S.G., Otsuka, T. and Merlino, G. (1997) Renal tubular hyperplasia, polycystic disease, and glomerulosclerosis in transgenic mice overexpressing hepatocyte growth factor/scatter factor. *Lab. Invest.*, **77**, 131–138.
17. Kim, E., Arnould, T., Sellin, L.K., Benzing, T., Fan, M.J., Gruning, W., Sokol, S.Y, Drummond, I. and Walz, G. (1999) The polycystic kidney disease 1 gene product modulates Wnt signaling. *J. Biol. Chem.*, **274**, 4947–4953.
18. He, T.-C., Sparks, A.B., Rago, C., Hermeking. H., Zawel, L., da Costa. L.T., Morin, P.J., Vogelstein, B. and Kinzler, K.W. (1998) Identification of c-MYC as a target of the APC pathway. *Science*, **281**, 1509–1512.
19. Holgado-Madruga, M., Emlet, D.R., Moscatello, D.K., Godwin, A.K. and Wong, A.J. (1996) A Grb2-associated docking protein in EGF- and insulin-receptor signalling. *Nature*, **379**, 560–564.
20. Weidner, K.M., Di Cesare, S., Sachs, M., Brinkmann, V., Behrens, J. and Birchmeier, W. (1996) Interaction between Gab1 and the c-Met receptor tyrosine kinase is responsible for epithelial morphogenesis. *Nature*, **384**, 173–176.
21. Lefebvre, A.M., Chen, I., Desreumaux, P., Najib, J., Fruchart, J.C., Geboes, K., Briggs, M., Heyman, R. and Auwerx, J. (1998) Activation of the peroxisome proliferator-activated receptor gamma promotes the development of colon tumors in C57BL/6J-APCMin/+ mice. *Nat. Med.*, **4**, 1053–1057.
22. Ohta, K., Endo. T., Haraguchi, K., Hershman, J.M. and Onaya, T. (2001) Ligands for peroxisome proliferator-activated receptor gamma inhibit growth and induce apoptosis of human papillary thyroid carcinoma cells. *J. Clin. Endocrinol. Metab.*, **86**, 2170–2177.

23. Kirby, M.L., Gale. T.F. and Stewart, D.E. (1983) Neural crest cells contribute to normal aorticopulmonary septation. *Science*, **220**, 1059–1061.
24. Wang, D., Iversen, J. and Strandgaard, S. (2000) Endothelium-dependent relaxation of small resistance vessels is impaired in patients with autosomal dominant polycystic kidney disease. *J. Am. Soc. Nephrol.*, **11**, 1371–1376.
25. Vanhoutte, P.M. and Mombouli, J.V. (1996) Vascular endothelium: vasoactive mediators. *Prog. Cardiovasc. Dis.*, **39**, 229–238.
26. Kirby, M.L., Turnage, K.L. 3rd. and Hays, B.M. (1985) Characterization of conotruncal malformations following ablation of 'cardiac' neural crest. *Anat. Rec.*, **213**, 87–93.
27. Conway, S.J., Bundy, J., Chen, J., Dickman, E., Rogers, R. and Will, B.M. (2000) Decreased neural crest stem cell expansion is responsible for the conotruncal heart defects within the splotch (Sp(2H))/Pax3 mouse mutant. *Cardiovasc. Res.*, **47**, 314–328.
28. Miller, J.R., Hocking, A.M., Brown, J.D. and Moon, R.T. (1999) Mechanism and function of signal transduction by the Wnt/β-catenin and Wnt/Ca2+ pathways. *Oncogene*, **18**, 7860–7872.
29. Gruber, P.J., Kubalak, S.W., Pexieder, T., Sucov, H.M., Evans, R.M. and Chien, K.R. (1996) RXR alpha deficiency confers genetic susceptibility for aortic sac, conotruncal, atrioventricular cushion, and ventricular muscle defects in mice. *J. Clin. Invest.*, **98**, 1332–1343.
30. Rosen, E.D. and Spiegelman, B.M. (2001) PPAR: a nuclear regulator of metabolism, differentiation, and cell growth. *J. Biol. Chem.*, **276**, 37731–37734.
31. Saadi-Kheddouci, S., Berrebi, D., Romagnolo, B., Cluzeaud, F., Peuchmaur, M., Kahn, A., Vandewalle, A. and Perret, C. (2001) Early development of polycystic kidney disease in transgenic mice expressing an activated mutant of the β-catenin gene. *Oncogene*, **20**, 5972–5981.
32. Sorenson, C.M., Padanilam, B.J. and Hammerman, M.R. (1996) Abnormal post-partum renal development and cystogenesis in the bcl-2$^{-/-}$ mouse. *Am. J. Physiol.*, **271**, F184–F193.
33. Sorenson, C.M. (1999) Nuclear localization of beta-catenin and loss of apical brush border actin in cystic tubules of bcl-2$^{-/-}$ mice. *Am. J. Physiol.*, **276**, F210–F217.
34. Huan, Y. and van Adelsberg, J. (1999) Polycystin-l, the *PKD1* gene product, is in a complex containing E-cadherin and the catenins. *J. Clin. Invest.*, **104**, 1459–1468.
35. Muthuswamy, S.K., Li, D., Lelievre, S., Bissell, M.J. and Brugge, J.S. (2001) ErbB2, but not ErbB1, reinitiates proliferation and induces luminal repopulation in epithelial acini. *Nat. Cell Biol.*, **3**, 785–792.
36. Sweeney, W.E., Chen, Y. Nakanishi, K., Frost, P. and Avner, E.D. (2000) Treatment of polycystic kidney disease with a novel tyrosine kinase inhibitor. *Kidney Int.*, **57**, 33–40.
37. Gonzalez-Perret, S., Kim, K., Ibarra, C., Damiano, A.E., Zotta, E., Batelli, M., Harris, P.C., Reisin, I.L., Arnaout, M.A. and Cantiello, H.F. (2001) Polycystin-2, the protein mutated in autosomal dominant polycystic kidney disease (ADPKD), is a Ca^{2+}-permeable nonselective cation channel. *Proc. Natl Acad. Sci. USA*, **98**, 1182–1187.
38. Koulen. P., Cai, Y., Geng, L., Maeda, Y, Nishimura, S., Witzgall, R., Ehrlich, B.E. and Somlo, S. (2002) Polycystin-2 is an intracellular calcium release channel. *Nat. Cell. Biol.*, **4**, 191–197.
39. Griffin, M.D., Torres, V.E., Grande, J.P. and Kumar, R. (1997) Vascular expression of polycystin. *J. Am. Soc. Nephrol.*, **8**, 616–626.
40. Ibraghimov-Beskrovnaya, O., Dackowski, W.R., Foggensteiner, L., Coleman, N., Thiru, S., Petry, L.R., Burn, T.C., Connors, T.D., Van Raay, T., Bradley, J. *et al.* (1997) Polycystin: *in vitro* synthesis, *in vivo* tissue expression, and subcellular localization identifies a large membrane-associated protein. *Proc. Natl Acad. Sci. USA*, **94**, 6397–6402.
41. Lohning, C., Nowicka, U. and Frischauf, A.M. (1997) The mouse homolog of PKD1: sequence analysis and alternative splicing. *Mamm. Genome*, **8**, 307–311.
42. Yagi, T., Ikawa, Y, Yoshida, K., Shigetani, Y, Takeda, N., Mabuchi, I., Yamamoto, T. and Aizawa, S. (1990) Homologous recombination at c-fyn locus of mouse embryonic stem cells with use of diphtheria toxin A-fragment gene in negative selection. *Proc. Natl Acad. Sci. USA*, **87**, 9918–9922.
43. Koera, K., Nakamura, K., Nakao, K., Miyoshi, J., Toyoshima, K., Hatta, T., Otani, H., Aiba, A. and Katsuki, M. (1997) K-ras is essential for the development of the mouse embryo. *Oncogene*, **15**, 1151–1159.
44. Ong, A.C., Harris, P.C., Davies, D.R., Pritchard, L., Rossetti, S., Biddolph, S., Vaux, D.J., Migone, N. and Ward, C.J. (1999) Polycystin-1 expression in PKD1, early-onset PKD1, and TSC2/PKD1 cystic tissue. *Kidney Int.*, **56**, 1324–1333.
45. Saito, Y., Yamagishi, T., Nakamura, T., Ohyama, Y., Aizawa, H., Suga, T., Matsumura, Y., Masuda, H., Kurabayashi, M., Kuro-o, M. *et al.* (1998) Klotho protein protects against endothelial dysfunction. *Biochem. Biophys. Res. Commun.*, **248**, 324–329.